Journal of Alloys and Compounds 509 (2011) 6184–6189

Contents lists available at ScienceDirect

Journal of Alloys and Compounds

journal homepage: www.elsevier.com/locate/jallcom

Activity determination in the alumina–dysprosia system by Knudsen effusion mass spectrometry

V.B. Motalov[a,1], M.F. Butman[b], L.S. Kudin[b], T. Markus[a,*]

[a] *Institute for Energy Research (IEF-2), Forschungszentrum Jülich GmbH, D-52425 Jülich, Germany*
[b] *Ivanovo State University of Chemistry and Technology, prosp. Engelsa 7, 153000 Ivanovo, Russia*

ARTICLE INFO

Article history:
Received 21 October 2010
Received in revised form 24 January 2011
Accepted 30 January 2011
Available online 6 April 2011

Keywords:
Al_2O_3–Dy_2O_3
Powders–gas phase reaction
Chemical properties
Lamp envelopes
Vaporization
Knudsen effusion mass spectrometry

ABSTRACT

The vaporization of Al–Dy–O mixtures has been investigated by the Knudsen effusion mass spectrometry technique. The saturated vapor has been found to consist of the atoms Al, O and the molecules AlO, Al_2O, DyO. At the initial stage the vaporization of Dy_2O_3 and Al_2O_3–Dy_2O_3 mixtures was found to be incongruent and accompanied by some loss of oxygen. An attainment of congruently vaporizing composition and equilibrium state takes quite a long time. The activities of binary oxides have been measured at $T = 2130$ K. The Gibbs energies and enthalpies have been derived for formation of the compounds $Dy_4Al_2O_9$, $DyAlO_3$ and $Dy_3Al_5O_{12}$ from sesquioxides.

1. Introduction

Alumina–lanthanide oxide systems (Al_2O_3–Ln_2O_3) are used in production of high quality alumina-rich glass and ceramics. To assess the thermodynamic stability and reactivity of these systems under various preparation, processing and operational conditions a consistent set of thermodynamic properties is required. Available information refers primarily to phase diagram characterization and solid phase equilibria study. Schneider et al. [1] reported on the existence of various compounds (perovskites, garnets and of other types) in Al_2O_3–Ln_2O_3 systems by X-ray diffraction technique. The systematic phase diagram characterization by X-ray and thermal analysis was undertaken in a series of works of Mizuno et al. (see, *e.g.* [2]). Wu and Pelton [3] carried out a critical assessment of the Al_2O_3–Ln_2O_3 systems through the technique of coupled thermodynamic-phase diagram analysis and calculated thermodynamic properties (enthalpies and entropies) of the various compounds and of the liquid oxide solutions as well as optimized phase diagrams. Le Floch et al. [4] reported on metastable solidification of $Ln_3Al_5O_{12}$ (Ln = Dy, Lu) garnets examined by differential thermal analysis (DTA). Gervias and Douy [5] reinvestigated solid phase transformation and melting of $Ln_4Al_2O_9$ (Ln = Gd, Dy) compounds by DTA and dilatometry. Solution calorimetry (SC) was applied to study the thermodynamics of phase equilibria for $LnAlO_3$ perovskites and $Ln_3Al_5O_{12}$ garnets in the investigation of Kanke and Navrotsky [6] and Cordfunke et al. [7]. Recently a new approach based on Pauling's concept of electronegativity was developed by Voňka and Leitner [8] for evaluation of the formation enthalpies of the $Ln_4Al_2O_9$, $LnAlO_3$, and $Ln_3Al_5O_{12}$ compounds.

Until now information on the thermodynamic activities of sesquioxides in the systems at high temperatures is missing. Such information is of particular significance in simulating the high pressure discharge metal halide lamps, in which the Al_2O_3–Ln_2O_3 systems are applied as sealing glasses. The formation of Ln–Al–oxide species occurs in the lamps due to corrosive reactions between the salt filling inside the discharge vessel and the burner wall made from alumina [9]. Technologically DyI_3 is among the most frequently used salts.

The phase diagram of the Al_2O_3–Dy_2O_3 system is shown in Fig. 1. Knowledge on thermodynamic properties of the compounds $Dy_4Al_2O_9$, $DyAlO_3$, $Dy_3Al_5O_{12}$ formed in this system is scanty and contradictory so far. Enthalpies of formation of these compounds were extensively studied by the two groups [6,7] with the use of SC technique. However these results are in conflict with each other.

The purposes of the present study are the measurements of individual oxide activities in alumina–dysprosia (Al_2O_3–Dy_2O_3) system and the determination of Gibbs energies of formation of compounds

---

[*] Corresponding author. Tel.: +49 02461 61 4470; fax: +49 02461 61 3699.
E-mail address: T.Markus@fz-juelich.de (T. Markus).
[1] On leave from Ivanovo State University of Chemistry and Technology, prosp. Engelsa 7, 153000 Ivanovo, Russia.

0925-8388/$ – see front matter © 2011 Elsevier B.V. All rights reserved.
doi:10.1016/j.jallcom.2011.01.166

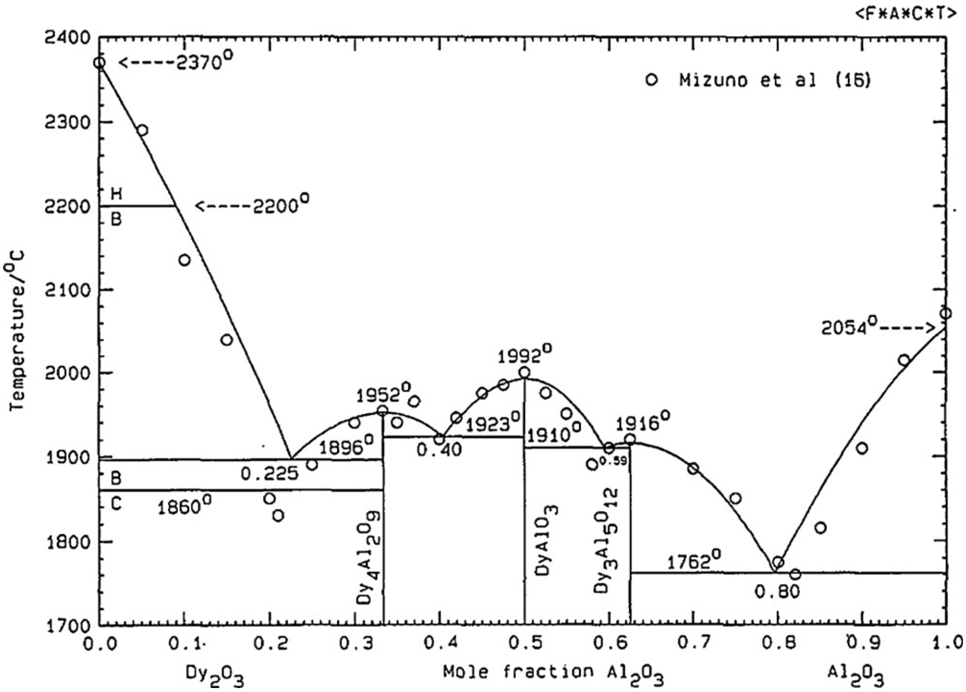

Fig. 1. Phase diagram of Al_2O_3–Dy_2O_3 system (taken from Ref. [3]).

from sesquioxides in the crystal phase by Knudsen effusion mass spectrometry (KEMS).

2. Experimental

2.1. Sample preparation and characterization

The starting materials used were dysprosium oxide (purity 99.9%, Rhone Poulenc, France) and aluminum oxide (high purity alumina, Baikowski, USA). Before use first these materials were dried at 800 °C for 16 h in air. To synthesize $Dy_4Al_2O_9$, $DyAlO_3$, and $Dy_3Al_5O_{12}$ mixtures the starting materials with the wanted stoichiometry were ground in heptane for 30 min in an agate ball mill, decanted, dried and prefired at 1400 °C in alumina crucibles for 2 h in air. Subsequently, the prefired powders were milled again in heptane and fired for a second time at 1600 °C in alumina crucibles for 6 h. This last milling and firing step were repeated.

The fired materials were analyzed with X-ray diffraction (XRD) to identify the crystalline phases. The measurements were performed with a PANalytical X'Pert Pro MPD diffractometer, equipped with a Cu X-ray source and an X'Celerator detector.

In sample $Dy_3Al_5O_{12}$ no other phase than $Dy_3Al_5O_{12}$ could be detected. In sample $Dy_4Al_2O_9$, besides the major phase $Dy_4Al_2O_9$, a trace of $DyAlO_3$ was detected. Sample $DyAlO_3$ contained the major phase $DyAlO_3$ and traces of $Dy_3Al_5O_{12}$, $Dy_{4.67}(SiO_4)_3O$ and $Dy_{4.8}Si_{2.8}Pb_{0.2}O_{13}$ phases. The contamination with silicon oxide could be explained because grounding was performed in agate.

For the vaporization experiments mixtures of the synthesized dysprosium aluminum oxides were used. These mixtures of Dy_2O_3–$Dy_4Al_2O_9$ (1/1), $Dy_4Al_2O_9$–$DyAlO_3$ (1/3), $DyAlO_3$–$Dy_3Al_5O_{12}$ (4/1) and $Dy_3Al_5O_{12}$–Al_2O_3 (1/4) were prepared by means of milling in heptane for 30 min in agate.

Upon annealing the samples in vacuum at the temperatures lower than experimental ones the silicate-containing impurities were completely removed. As an evidence for this conclusion, Fig. 2 represents the XRD patterns of the synthesized $DyAlO_3$ before annealing (a) and of the quenched mixture (42 mol.% Al_2O_3) (b).

2.2. KEMS measurements

The vaporization experiments were carried out by using a substantially modified magnetic sector field single-focusing mass spectrometer of the type CH5 (supplied by Varian MAT Bremen, Germany) equipped with a Knudsen cell assembly. Knudsen cells made of tungsten and lined completely with iridium were used. The Knudsen cell is heated by electron bombardment and the vapor effusing through a channel type orifice (diameter: 0.3 mm) was ionized by electron impact. The ions produced were accelerated under a negative potential of 6000 V. The ion intensities were measured by secondary electron multiplier, Faraday cap or a counting system, depending on the ion intensity. More details about the instrument are given elsewhere [10]. For ionizing the vapor species, electrons with an emission current of 200 μA and with an energy of 27 eV were used. The temperature of the Knudsen cell was measured in a blackbody hole located close to and below the bottom of the Knudsen cell. An automatic infrared digital pyrometer (Dr. Georg Maurer GmbH, Kohlberg, Germany) which was calibrated against the melting points of silver, gold, and nickel was used for temperature measurements. The accuracy of the temperature measurement is considered to be within ±10 K. The electron energy scale was calibrated against the first ionization energies of pure metals [11].

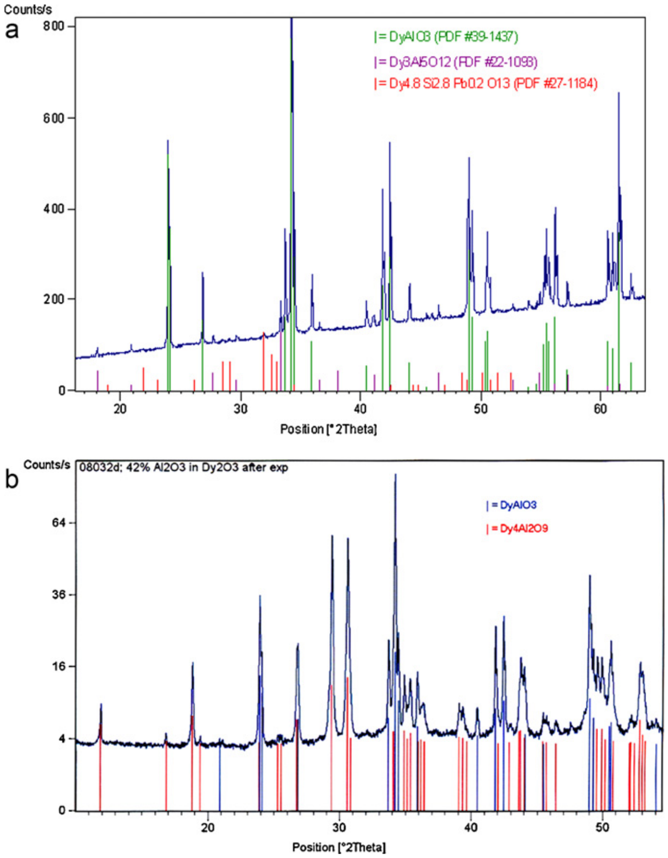

Fig. 2. XRD patterns of $DyAlO_3$ sample before HTMS experiment (a) and of the quenched mixture $(Al_2O_3)_{0.42}$–$(Dy_2O_3)_{0.58}$ after the experiment (b).

Table 1
Ion species registered in mass spectra and appearance energies, *AE* (eV).[a]

Al_2O_3	Al^+ (5.7), O^+ (13.7), AlO^+ (9.8), Al_2O^+ (7.9)
Dy_2O_3	Dy^+ (6.1), O^+ (13.8), DyO^+ (6.2), Dy^{++}
Al_2O_3–Dy_2O_3[b]	Al^+ (6.2), O^+ (13.9), AlO^+ (10.0), Al_2O^+ (8.1), Dy^+ (6.0), DyO^+ (6.0), Dy^{2+}

[a] The uncertainties in *AE* values are assessed to be ±0.5 eV. Ionization efficiency was not investigated for Dy^{2+} due to low peak intensity.

[b] The ion species listed are the same for both studied compositions of the $(Al_2O_3)_x$–$(Dy_2O_3)_{1-x}$ system ($x = 0.42$, 0.56); the appearance energies were measured for $x = 0.42$.

3. Results and discussion

3.1. Mass spectra and vapor composition

In the electron-impact-ionization mass spectra the ions listed in Table 1 have been detected in the temperature ranges of 1968–2238 K (Al_2O_3), 1951–2290 K (Dy_2O_3), and 2037–2210 K (Al_2O_3–Dy_2O_3 system). As one can see, the mass spectrum in the case of the system Al_2O_3–Dy_2O_3 was qualitatively the combination of those of individual oxides. No evidence of presence of heterocomplex ions (for instance, $DyAlO^+$) in the mass spectrum of the system was obtained. The ion species in the mass spectrum of pure Al_2O_3 are in agreement with the data of earlier mass spectrometric studies [12–19]. In Refs. [13,17–19] it is reported on the detection of $Al_2O_2^+$ and AlO_2^+ ions at temperatures higher than ours. The mass spectrum of pure Dy_2O_3 agrees with those reported earlier [20–22], for other lanthanide sesquioxides. In these spectra the Ln^+, LnO^+ ions are predominant.

Ion attribution to the neutral precursors was done by analysis of the ion appearance energies (Table 1) determined by the linear extrapolation method of the near-threshold segments of the ionization efficiency curves (IEC). The appearance energies of ions in mass spectra of pure oxides agree within the error of measurement with the results [12,13,15–19,23] of the earlier mass spectrometric determinations. The *AE* values are seen to be close for the pure oxides and the system and indicate that at low electron energies all the ions detected are parent ions produced by direct ionization of the respective atoms (Al, O, Dy) and molecules (AlO, Al_2O, DyO). In addition, no obvious breaks indicating fragmentation contributions at higher ionizing electron energy were revealed from IEC's shape analysis. Thus one can neglect the dissociative ionization of polyatomic species for both the pure oxides and the system. In order to check this conclusion for the energy of 27 eV used in the present study, an experiment with vaporization of pure Al_2O_3 under reducing conditions (when adding a small quantity of Ta to the sample) was performed. Figs. 3 and 4 respectively show the comparison of ion current ratios and equilibrium constants of the gas-phase reaction $Al_2O = Al + AlO$ expressed by ion currents measured under neutral and reducing conditions. It can be seen that in spite of considerable differences between the ion current ratios in the neutral and reducing vaporization conditions (about 3, 2.5 and 9 times for Al^+/AlO^+, Al^+/Al_2O^+ and AlO^+/Al_2O^+, respectively) the values of equilibrium constant remain practically unchanged thus confirming the fragmentation to be negligible.

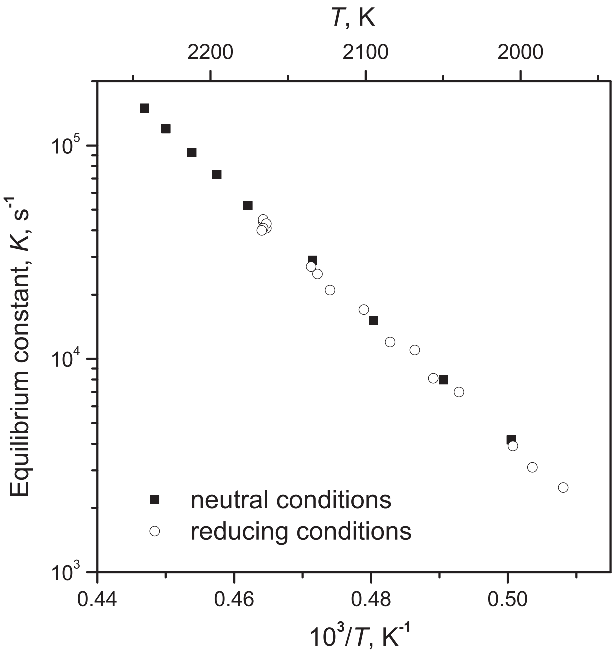

Fig. 4. Equilibrium constant expressed by ion currents for the reaction $Al_2O(g) = Al(g) + AlO(g)$.

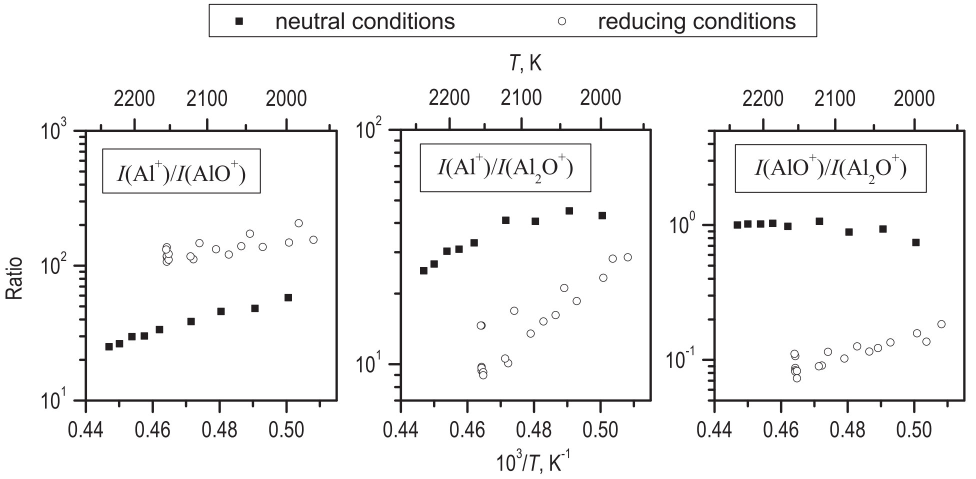

Fig. 3. Ion current ratios on vaporization of Al_2O_3.

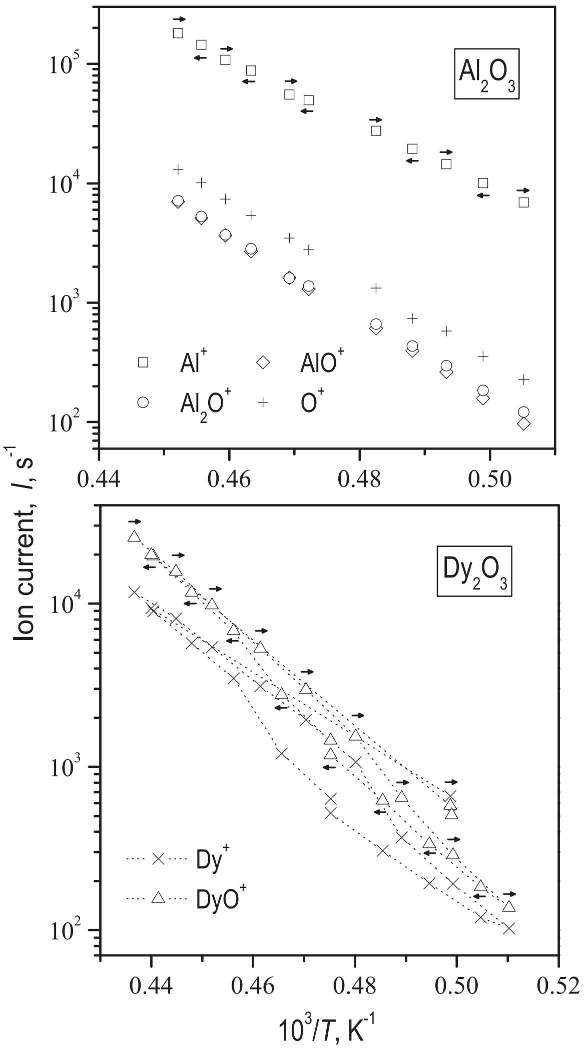

Fig. 5. Temperature dependences of ion currents (cooling and heating cycles are shown with arrows above an below points, respectively).

3.2. *Attainment of the equilibrium*

The temperature dependences of ion currents in the case of pure sesquioxides are shown in Fig. 5. It can be seen that the ion currents in the experiment with Al_2O_3 are well reproducible in the cooling–heating cycles. In contrast, the temperature dependence for Dy_2O_3 is of hysteresis type. This observation compelled us to suspect that there are some difficulties for equilibrium attainment within a Knudsen cell.

To study the possible changes in ion currents with time for each composition of the $(Al_2O_3)_x$–$(Dy_2O_3)_{1-x}$ system (x = 0.42, 0.56) and for pure sesquioxides, long-term isothermal vaporization runs were carried out at T = 2130 K (Fig. 6). The instrument was allowed to stabilize for ∼1 h before the initial ion current measurement. The fluctuations in the temperature over the isothermal runs were no more than ±1 K. Vaporization of pure Al_2O_3 was carried out before and after every long-term isothermal run in order to ensure the reproducibility of sensitivity. It can be seen that in the case of Dy_2O_3 and the Al_2O_3–Dy_2O_3 system, the ion currents change drastically at the initial vaporization stage, whereas those in the case of Al_2O_3 demonstrate constancy with time. An apparent steady-state, which may be characterized as congruent vaporization, is achieved in quite long time intervals: about 6 h for Dy_2O_3 and at least 30 h for the Al_2O_3–Dy_2O_3 system. At the first stage the vaporization of Dy_2O_3 and Al_2O_3–Dy_2O_3 is incongruent with high fraction of oxygen in the vapor, which decreases with time. The other ion currents stay almost constant (Dy_2O_3) or change at opposite trend with $I(O^+)$ after going through a minimum (Al_2O_3–Dy_2O_3). The observed changes reflect a gradual approach to congruently vaporizing composition. The formation of the congruently vaporizing oxygen-deficient phases $R_2O_{3-\delta}$ (R is lanthanide) with a small extent of deviation from stoichiometry ($\delta \sim 0.005$–0.02) under the conditions of high temperature vaporization in vacuum was reported earlier [22]. Since our XRD results did not reveal any new phases in the samples after vaporization within the sensitivity limits (see Section 2.1), the changes in ion currents observed may be attributed similarly to the defect formation process. Another reason, which might explain the initial evolution of ion currents, stems from an expected aging of the samples at early stages of sintering like for instance rapid reaction of smaller particles and their disappearance as well as evolution of the reactive surfaces [24].

Table 2
Activity, a^a, of individual sesquioxides in $(Al_2O_3)_x$–$(Dy_2O_3)_{1-x}$ system and Gibbs energy of formation, $-\Delta_{ox}G^\circ$ (kJ mol^{-1})^a, of mixed compounds from sesquioxides at 2130 K.

Property	Reaction	Composition	
		x = 0.42	x = 0.56
a_i			
$i = Al_2O_3$	(1)	0.039 ± 0.008	0.233 ± 0.047
	(2)	0.029 ± 0.009	0.243 ± 0.073
	Average	0.034 ± 0.006	0.238 ± 0.040
$i = Dy_2O_3$	(3)	0.100 ± 0.020	0.011 ± 0.002
$-\Delta_{ox}G_i^o$			
$i = Dy_4Al_2O_9$		141.4 ± 10.6	
$i = DyAlO_3$		50.3 ± 3.5	52.6 ± 3.5
$i = Dy_3Al_5O_{12}$			183.2 ± 14.2

[a] The overall uncertainty given with '±' sign is estimated on the base of run-to-run reproducibility (∼5%) of sensitivity constant of our instrument.

To examine an attainment of equilibrium at different stages of isothermal vaporization the equilibrium constant K of the gas phase reaction $Al_2O(g) = Al(g) + AlO(g)$ was calculated and plotted in Fig. 7 as a function of time. One can see that in each run with the system a strong deviation of K at the initial vaporization stage is observed. Eventually the values of K approach within the experimental errors to that measured for Al_2O_3 thus demonstrating that the steady-state stages of isothermal evaporation are equilibrium ones. Additional evidence to this inference is provided in the next section.

3.3. *Thermodynamic properties*

The activities of Al_2O_3 and Dy_2O_3 in the Al_2O_3–Dy_2O_3 system at 2130 K were derived considering the following reactions:

$$[Al_2O_3] + Al = 3AlO, \quad a_{Al_2O_3} = \frac{I_s^3(AlO^+)/I_s(Al^+)}{I_o^3(AlO^+)/I_o(Al^+)}; \tag{1}$$

$$[Al_2O_3] + Al_2O = 4AlO, \quad a_{Al_2O_3} = \frac{I_s^4(AlO^+)/I_s(Al_2O^+)}{I_o^4(AlO^+)/I_o(Al_2O^+)}; \tag{2}$$

$$[Dy_2O_3] + Dy = 3DyO, \quad a_{Dy_2O_3} = \frac{I_s^3(DyO^+)/I_s(Dy^+)}{I_o^3(DyO^+)/I_o(Dy^+)}. \tag{3}$$

(Crystal state is denoted by brackets; the symbols 's' and 'o' denote the measurements made in the system and in the pure oxides, respectively.) Oxygen-containing reactions were not used for the activity evaluation due to significant interfering background ion currents at m/e = 16. The activities, a, are listed in Table 2. The a values for Al_2O_3 obtained from reactions (1) and (2) agree well.

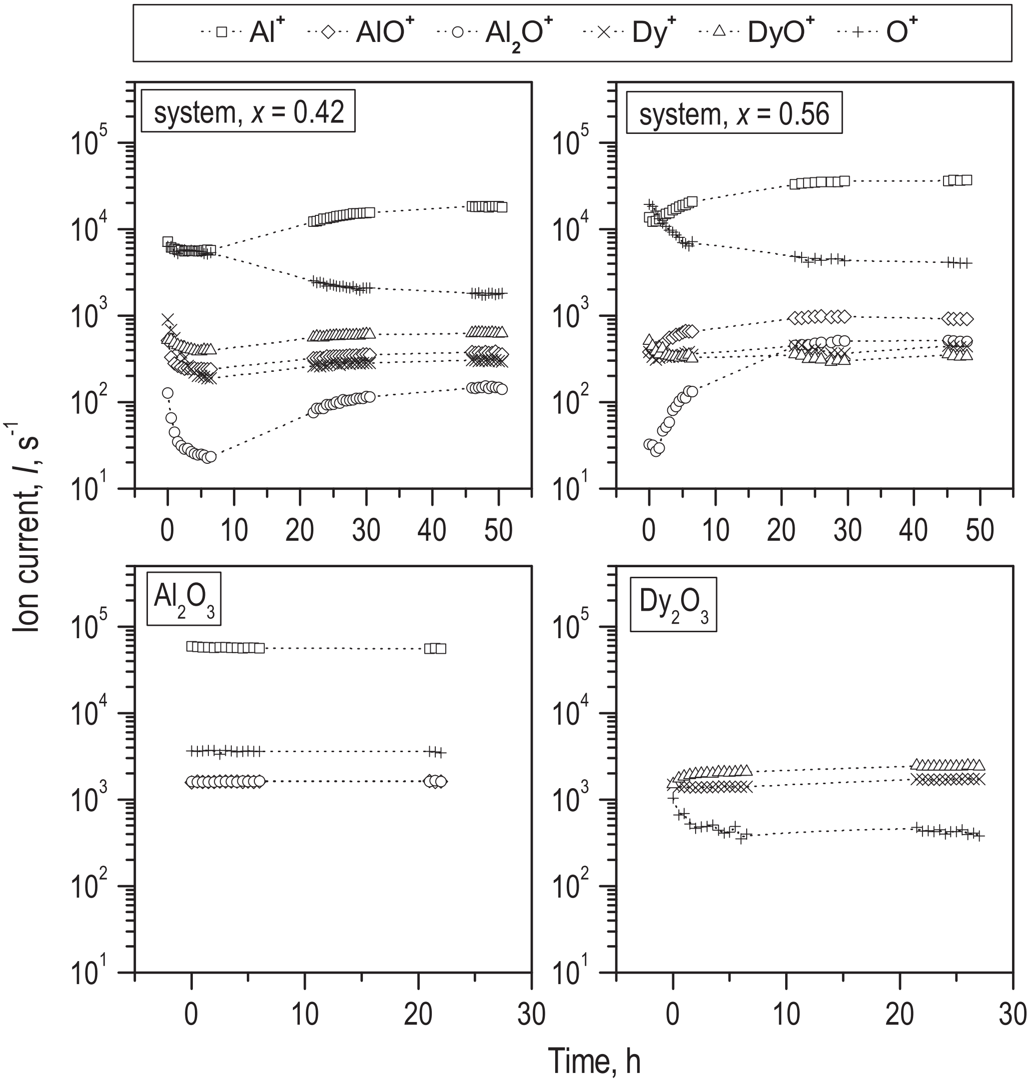

Fig. 6. Time dependencies of ion currents in long-term isothermal experiments on vaporization of pure sesquioxides and $(Al_2O_3)_x$–$(Dy_2O_3)_{1-x}$ system ($T = 2130$ K).

According to the phase diagram (Fig. 1) the individual crystal compounds are present in the $(Al_2O_3)_x$–$(Dy_2O_3)_{1-x}$ system at 2130 K: $Dy_4Al_2O_9$ ($x = 0.42$), $DyAlO_3$ ($x = 0.42, 0.56$) and $Dy_3Al_5O_{12}$ ($x = 0.56$). To calculate the Gibbs energies for the formation of these compounds from sesquioxides the following solid-state reactions were considered:

$$Al_2O_3 + 2Dy_2O_3 = Dy_4Al_2O_9, \quad \Delta_{ox}G^o_T = RT\ \ln(a_{Al_2O_3} \cdot a^2_{Dy_2O_3}); \tag{4}$$

$$0.5Al_2O_3 + 0.5Dy_2O_3 = DyAlO_3, \quad \Delta_{ox}G^o_T = RT\ \ln(a^{0.5}_{Al_2O_3} \cdot a^{0.5}_{Dy_2O_3}); \tag{5}$$

$$2.5Al_2O_3 + 1.5Dy_2O_3 = Dy_3Al_5O_{12} \quad (6), \quad \Delta_{ox}G^o_T = RT\ \ln(a^{2.5}_{Al_2O_3} \cdot a^{1.5}_{Dy_2O_3}). \tag{6}$$

The results are listed in Table 2. It can be seen that the Gibbs energies of $DyAlO_3$ determined from measurements in the different fields of the phase diagram ($x = 0.42, 0.56$) are in good agreement thus supporting the inference made above on the correspondence of the steady-states of vaporization to the equilibrium ones.

The Gibbs energies resulted as (kJ mol^{-1}): −141.4 ± 10.6 ($Dy_4Al_2O_9$), −51.5 ± 2.5 ($DyAlO_3$) and −183.2 ± 14.2 ($Dy_3Al_5O_{12}$) do not contradict the respective values −134.0, −56.7 and −211.5 evaluated for $T = 2130$ K from the enthalpies and entropies assessed by Wu and Pelton [3], which were considered to be temperature independent. In order to compare our results with the literature data [3,6,7] on formation enthalpies of the compounds from sesquioxides we derived $\Delta_{ox}H$ values from the Gibbs energies determined using the entropies from Ref. [3]. The enthalpies are compared (Table 3) under assumption [3,8] that $\Delta_{ox}H(T) = \Delta_{ox}H(298.15)$. It should be noticed that the heat capacities of the $Dy_4Al_2O_9$, $DyAlO_3$ and $Dy_3Al_5O_{12}$ compounds were measured by Cordfunke et al. [7] in the temperature range of 10–930 K. However we did not use these data for reducing our high temperature enthalpies to $T = 298.15$ K due to the large extrapolation involved on the one hand, and poor reliability of the data [7], on the other hand (see discussion below).

It can be seen from Table 3 that in case of $Dy_4Al_2O_9$ and $DyAlO_3$ the enthalpies of different authors agree satisfactorily except for the data [7], which are systematically higher in absolute value for all the compounds under consideration. It is noteworthy that (1) the data of Refs. [6,7] were obtained by the same method (solution calorimetry) but with different solvents; (2) the data of Ref. [8] based on Pauling's concept of electronegativity were fitted to

Table 3
Enthalpies of formation of mixed compounds from sesquioxides, $-\Delta_{ox}H^\circ$ (kJ mol^{-1}).[a]

Ref., method	$Dy_4Al_2O_9$	$DyAlO_3$	$Dy_3Al_5O_{12}$
This work, KEMS	87.5 ± 10.6	24.1 ± 2.5	162.6 ± 14.2
Kanke and Navrotsky [6], SC		21.4 ± 2.2	97.7 ± 6.2
Cordfunke et al. [7][b], SC	228.5 ± 7.5	91.0 ± 7.8	219.4 ± 10.9
Wu and Pelton [3], assessment	80.1	29.3	190.9
Voňka and Leitner [8], estimation	75.7	28.4	106.5

[a] The errors are overall uncertainties (this work, Ref. [7]) or standard deviations (Ref. [6]).

[b] The standard formation enthalpies $\Delta_f H^\circ$ (298.15 K) [7] of the compounds were combined with $\Delta_f H^\circ$ (Al_2O_3, cr, 298.15 K) = −1675.7 ± 1.3 kJ mol^{-1} (Ref. [25]) and $\Delta_f H^\circ$ (Dy_2O_3, cr, 298.15 K) = −1863.4 ± 5.0 kJ mol^{-1} (Ref. [26]) in order to derive the $\Delta_{ox}H^\circ$ values.

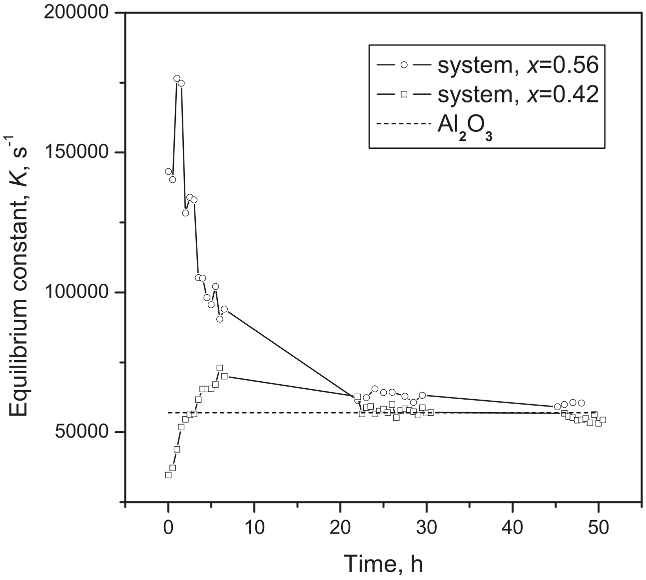

Fig. 7. Time dependencies of equilibrium constant *K* expressed by ion currents of the reaction $Al_2O(g) = Al(g) + AlO(g)$ (*T* = 2130 K).

experimental values of Ref. [6] and therefore cannot be considered as truly independent ones. The formation enthalpies of $Dy_3Al_5O_{12}$ are scattered in the range of about 120 kJ mol^{-1} with our value of −162.6 kJ mol^{-1} falling in its middle.

4. Conclusions

Vaporization processes in Al–Dy–O mixtures have been investigated by the Knudsen effusion mass spectrometry technique for the first time. The saturated vapor has been found to consist of the atoms Al, O and molecules AlO, Al_2O, and DyO. At the initial stage the vaporization of Dy_2O_3 and Al_2O_3–Dy_2O_3 system is incongruent and accompanied by some loss of oxygen. An attainment of congruently vaporizing composition and equilibrium state takes quite a long time. Thermodynamic treatment of the data is based on the approach [22] that slight deviation from stoichiometry due to oxygen deficiency does not affect significantly the thermodynamic characteristics. The activities of binary oxides have been measured in the $(Al_2O_3)_x$–$(Dy_2O_3)_{1-x}$ system (x = 0.42, 0.56) at *T* = 2130 K. The Gibbs energies and enthalpies have been calculated for reactions of formation of the mixed compounds $Dy_4Al_2O_9$, $DyAlO_3$ and $Dy_3Al_5O_{12}$ from the constituent sesquioxides.

Acknowledgements

The authors are very grateful to Philips Eindhoven for the financial support of this study and the preparation of the samples.

References

[1] S.J. Schneider, R.S. Roth, J.L. Waring, J. Res. Natl. Bur. Stand. Sect. A 65 (1961) 345–374.
[2] M. Mizuno, T. Yamada, T. Noguchi, Yogyo-Kyokai-Shi 86 (1978) 360–364.
[3] P. Wu, A.D. Pelton, J. Alloys Compd. 179 (1992) 259–287.
[4] S. Le Floch, J.C. Rifflet, J. Coutures, M. Gervais, J.P. Coutures, Mater. Sci. Eng. A 173 (1993) 185–187.
[5] M. Gervias, A. Douy, Mater. Sci. Eng. B 38 (1996) 118–121.
[6] Y. Kanke, A. Navrotsky, J. Solid State Chem. 141 (1998) 424–436.
[7] E.H.P. Cordfunke, A.S. Booij, R.R. van der Laan, Thermochemische eigenschappen van de dysprosium aluminaten $DyAlO_3$, $Ln_4Al_2O_9$, $Ln_3Al_5O_{12}$. Report of Energy research center of Netherland (ECN-C-96-010), 1996.
[8] P. Voňka, J. Leitner, J. Solid State Chem. 182 (2009) 744–748.
[9] M. Born, T. Markus, Lect. Notes Phys. 670 (2005) 399–423.
[10] K. Hilpert, K. Ruthardt, Ber. Bunsenges Phys. Chem. 91 (1987) 724–731.
[11] K. Hilpert, K.A. Gingerich, Int. J. Mass Spectrom. Ion Phys. 47 (1983) 247–250.
[12] G. De Maria, J. Drowart, M.G. Inghram, J. Chem. Phys. 30 (1959) 318–319.
[13] J. Drowart, G. DeMaria, R.P. Burns, M.G. Inghram, J. Chem. Phys. 32 (1960) 1366–1372.
[14] R.P. Burns, A.J. Jason, M.G. Inghram, J. Chem. Phys. 40 (1964) 2739–2740.
[15] R.P. Burns, J. Chem. Phys. 44 (1966) 3307–3319.
[16] M. Farber, R.D. Srivastava, O.M. Uy, J. Chem. Soc. Faraday Trans. I68 (1972) 249–258.
[17] R.C. Paule, High Temp. Sci. 8 (1976) 257–266.
[18] A.D. Chervonyi, V.A. Piven, O.E. Kashireninov, G.B. Manelis, High Temp. Sci. 9 (1977) 99–108.
[19] P. Ho, R.P. Burns, High Temp. Sci. 12 (1980) 31–39.
[20] M.B. Panish, J. Chem. Phys. 34 (1961) 1079–1080.
[21] J. Kordis, K.A. Gingerich, J. Chem. Phys. 66 (1977) 483–491.
[22] D. White, D.N. Walsh, L.L. Ames, H.W. Goldstein, Thermodynamics of Nuclear Materials, IAEA, Vienna, 1962, pp. 417–443.
[23] R.J. Ackermann, E.G. Rauh, R.J. Thorn, J. Chem. Phys. 65 (1976) 1027–1031.
[24] S. Baud, F. Thevenot, C. Chatillon, J. Eur. Ceram. Soc. 23 (2003) 9–18.
[25] L.V. Gurvich, I.V. Veitz, V.A. Medvedev, et al., in: V.P. Glushko (Ed.), Termodinamicheskie svoistva individual'nykh veshchestv (Thermodynamic Properties of Individual Substances), vols.1–4, 3rd ed., Nauka, Moscow, 1978–1984.
[26] E.H.P. Cordfunke, R.J.M. Konings, Thermochim. Acta 375 (2001) 65–79.